PROCEEDINGS OF SCIENCE

Global Fits of simplified dark matter models with GAMBIT

Christopher Chang*, on behalf of the GAMBIT Community

School of Mathematics and Physics, The University of Queensland,
St Lucia, Brisbane, Australia

E-mail: christopher.chang@uqconnect.edu.au

Dark matter candidates can arise from a wide range of extensions to the Standard Model. Simplified models with a small number of new particles allow for the optimisation and interpretation of dark matter and collider experiments, without the need for a UV-complete theory. In this talk, I will discuss the results from a recent GAMBIT study of global constraints on vector-mediated simplified dark matter models. I will cover several models with differing spins of the dark matter candidate.

DISCRETE 2022
Baden-Baden, Germany
7–11 Nov 2022

PoS(DISCRETE2022)021

1. Introduction

A number of astrophysical and cosmological observations suggest that the Standard Model (SM) should be extended to include a heavy dark matter (DM) candidate [2, 5, 6]. Simplified dark matter models describe effective DM interactions and differ from traditional effective field theories as they do not integrate out the particle that mediates exchanges between DM and the SM. In this way, they are a useful tool for studying how both low and high-energy experiments probe Beyond-the-Standard Model (BSM) physics.

We consider three simplified DM models with a spin-1 vector mediator in this work [1], where each model differs by the nature of the DM candidate:

- spin 0 (complex scalar)
- spin $\frac{1}{2}$ (Dirac fermion)
- spin $\frac{1}{2}$ (Majorana fermion)

We assume that DM is a singlet under the SM gauge group and that it should be odd under a new $\mathbb{Z}_2$ symmetry to ensure absolute stability. Scenarios with a real spin-1 mediator could typically arise when the SM gauge group is extended by an abelian symmetry group. We restrict the models to purely coupling to quarks to avoid strong di-lepton searches [3]. If these were to be included, the likelihood surface would give preference to parameter regions where the branching fraction into leptons is low. We fix all quark couplings to the mediator to be equal to assume Minimal Flavour Violation and to reduce the number of parameters scanned over in the global fit. Lastly, we assume that none of the models would give observable mixing between any SM particles and the mediator, which is required in order to reinterpret many experimental results to constrain BSM physics.

1.1 Scalar DM

The Lagrangian density of the scalar DM simplified model is

$$\begin{aligned}\mathcal{L}_{\rm BSM} =& \partial_\mu \phi^\dagger \partial^\mu \phi - m_{\rm DM}^2 \phi^\dagger \phi - \frac{1}{4} F'_{\mu\nu} F'^{\mu\nu} - \frac{1}{2} m_{\rm M}^2 V_\mu V^\mu \\ &+ g_{\rm q} V_\mu \bar{q} \gamma^\mu q + i g_{\rm DM}^{\rm V} V_\mu \left(\phi^\dagger (\partial^\mu \phi) - (\partial^\mu \phi^\dagger) \phi \right),\end{aligned} \tag{1}$$

where V_μ is the mediator particle, $F'_{\mu\nu}$ is the mediator strength tensor and ϕ is the scalar DM candidate. To prevent a vanishing $g_{\rm DM}^{\rm V}$, the scalar DM must be a complex scalar. There are four free model parameters: the two particle masses, the DM coupling $g_{\rm DM}^{\rm V}$ and the quark coupling $g_{\rm q}$.

1.2 Dirac DM

The Lagrangian density of the Dirac DM simplified model is

$$\begin{aligned}\mathcal{L}_{\rm BSM} =& i \bar{\chi} \gamma^\mu \partial_\mu \chi - m_{\rm DM} \bar{\chi} \chi - \frac{1}{4} F'_{\mu\nu} F'^{\mu\nu} - \frac{1}{2} m_{\rm M}^2 V_\mu V^\mu \\ &+ g_{\rm q} V_\mu \bar{q} \gamma^\mu q + V_\mu \bar{\chi} (g_{\rm DM}^{\rm V} + g_{\rm DM}^{\rm A} \gamma^5) \gamma^\mu \chi \,,\end{aligned} \tag{2}$$

where χ is the Dirac fermion DM candidate and the other fields are given as before. We allow both the vector and axial-vector mediator DM couplings to vary independently, such that this model has five free parameters (two masses and three couplings).

This model suffers from perturbative unitarity violation in the case of a nonzero axial-vector mediator DM coupling which could be avoided by the inclusion of a dark Higgs boson to the theory. We reject parameter points that do not satisfy the unitarity bound of Ref. [3].

$$m_{\rm DM} \leq \sqrt{\frac{\pi}{2}} \frac{m_{\rm M}}{g^{\rm A}_{\rm DM}}. \tag{3}$$

1.3 Majorana DM

The Lagrangian density of the Majorana DM simplified model is

$$\begin{aligned} \mathcal{L}_{\rm BSM} =& \frac{1}{2} i\bar{\psi}\gamma^\mu \partial_\mu \psi - \frac{1}{2} m_{\rm DM} \bar{\psi}\psi - \frac{1}{4} F'_{\mu\nu} F'^{\mu\nu} - \frac{1}{2} m^2_{\rm M} V_\mu V^\mu \\ &+ g_{\rm q} V_\mu \bar{q}\gamma^\mu q + \frac{1}{2} g^{\rm A}_{\rm DM} V_\mu \bar{\psi}\gamma^5\gamma^\mu\psi. \end{aligned} \tag{4}$$

Pure vector couplings to the mediator are forbidden in this model, and so only an axial-vector mediator-DM coupling ($g^{\rm A}_{\rm DM}$) is present and the model has four free parameters. This model will also face the perturbative unitarity violation described in section 1.2, and also reject any parameter points that do not satisfy the bound above.

2. Constraints

We constrain each model with likelihoods from DM direct and indirect detection experiments, the measured DM relic abundance and collider searches with both ATLAS and CMS experiments. For full details on the implementation of each of these likelihoods, we refer the reader to Ref. [1]. For the Dirac DM model, we additionally reject any points in parameter space that violate the bound of eq (3).

3. Results

We performed GAMBIT scans of each model using the differential evolution sampler Diver v1.0.4 [4]. The results are presented as profile likelihood maps in the plane of the two BSM particle masses. Up to four individual scans were performed for each model, with the DM relic abundance taken as either an upper limit or a two-sided measurement, and with the collider likelihood either capped [1] or uncapped. Only a subset of these results is shown in this talk.

The scan ranges for each model and nuisance parameter are listed in Table 1. To prevent fine-tuning or large hierarchies between different couplings, we prevent the lower limit of the couplings from being too low.

Parameters	**Range**
DM mass, $m_{\rm DM}$	[50, 10000] GeV
Mediator mass, $m_{\rm M}$	[50, 10000] GeV
quark-mediator coupling, $g_{\rm q}$	[0.01, 1.0]
mediator-DM coupling (vector), $g^{\rm V}_{\rm DM}$	[0.01, 3.0]
mediator-DM coupling (axial vector), $g^{\rm A}_{\rm DM}$	[0.01, 3.0]
Nuisance Parameters	**Value** ($\pm 3\sigma$ range)
Local DM density, ρ_0	[0.2, 0.8] GeV cm^{-3}
Most probable speed, $v_{\rm peak}$	240(24) km s^{-1}
Galactic escape speed, $v_{\rm esc}$	528(75) km s^{-1}

Table 1: Scan ranges for each model or nuisance parameter. The Dirac DM model is the only one containing the axial-vector coupling $g^{\rm A}_{\rm DM}$.

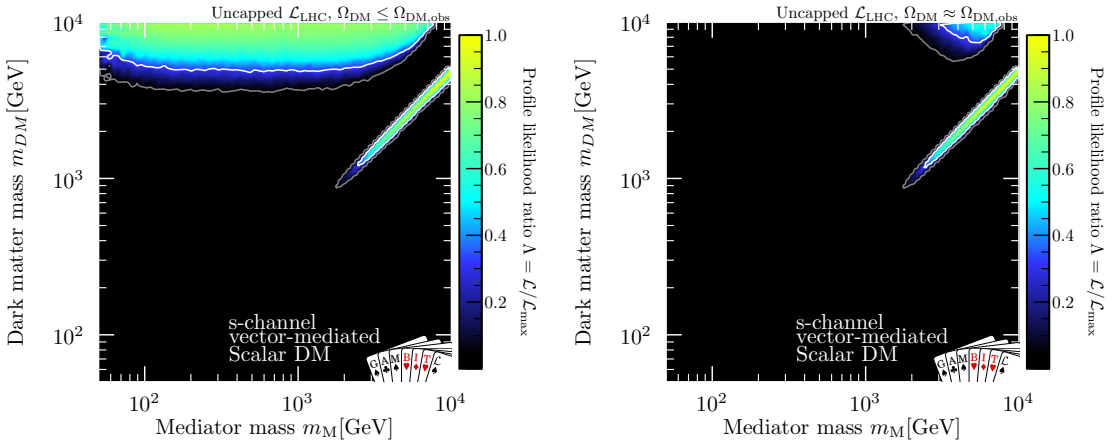

Figure 1: Profile likelihood for the scalar DM model. The model is allowed to underpredict the observed relic abundance (left) or to saturate the relic abundance (right). 1σ contours are shown in white whilst 2σ contours are shown in grey.

3.1 Scalar DM

We show the results of global scans of the scalar DM model in Figure 1. Capped collider results are not shown, since any regions that might show a preference in the monojet likelihoods are well excluded by other likelihoods.

Two separate regions can be clearly seen in the exclusion contours. These are due to the two different DM annihilation channels: into a pair of quarks when $m_{\rm M} \approx 2m_{\rm DM}$, and into a pair of mediators when $m_{\rm DM} > m_{\rm M}$. An increased DM annihilation cross-section in these regions results in an underprediction of the DM relic density, weakening the strength of limits from Planck relic abundance measurements and direct detection experiments. Requiring that the relic abundance is

[1]In this procedure, the likelihood is allowed to be no higher than a SM background only fit. See section 3.4 of Ref. [1] for more details.

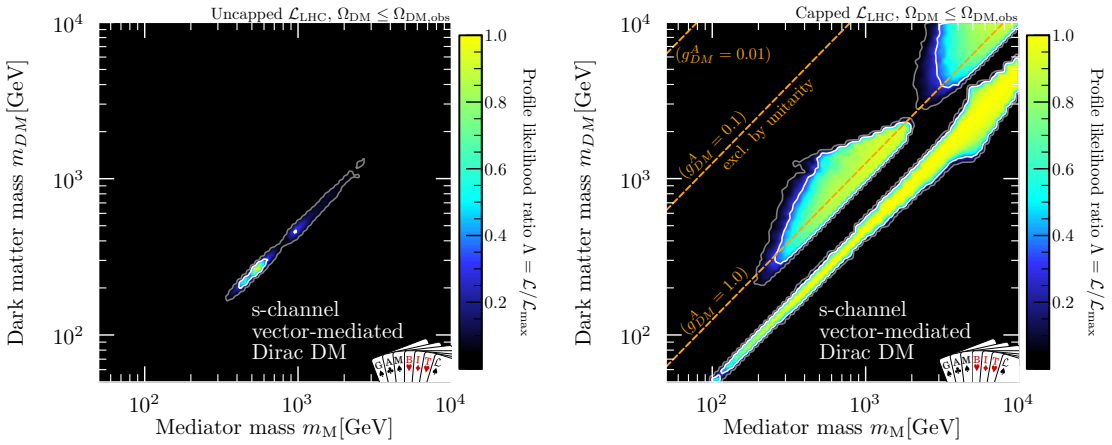

Figure 2: Profile likelihood for the Dirac fermion DM model where the model is allowed to underpredict the observed relic abundance. The collider likelihood is either capped (right) or left uncapped (left). 1σ contours are shown in white whilst 2σ contours are shown in grey.

saturated shrinks the size of the surviving region to exclude much of the off-resonance region for mediator masses below 2 TeV.

The model is most preferred along the resonance region and toward higher masses toward the boundaries of the scan parameters. For increasing mediator mass, the strength of the effective coupling for the non-relativistic operator decreases. At the very boundaries, the predicted signal at DM experiments is small enough that the magnitude of the profile likelihood is not expected to change significantly if the scan boundaries were extended.

3.2 Dirac DM

We show the profile likelihood surface for the Dirac fermion DM model in Figure 2 when applying the Planck measurement as an upper bound. The left panel shows that there is a predicted preference over the Standard Model for DM masses around 200–300 GeV, along the resonance region. Small fluctuations in collider searches are known to give weak preference over the Standard Model, however, this is being exacerbated by the CMS monojet search. The simplified likelihood for this search suffers from an artifact from the analysis control region fit. The CMS collaboration found that a joint fit of control and signal regions would most prefer no DM signal, however the background prediction from the control region fit underpredicts the expected mono-jet events in the 2018 section of the data. This may be seen in Figure 3, which shows the best fit-point for the Dirac DM model, and how this compares to the background predictions for this CMS analysis. Although the 2018 portion of the signal regions will give a preference toward a non-zero DM signal, this will not be entirely fit without producing a poor fit in the 2016 and 2017 signal regions.

Figure 2 (right) shows how the likelihood surface changes when the collider likelihood is capped, and these small fluctuations are assumed to arise from statistical noise. The allowed surface is split into three distinct regions. The reason that the off-resonance region is split in two is due to the combined effect of direct detection likelihoods and unitarity violation. To escape unitarity bounds, the model prefers small $g^{\rm A}_{\rm DM}$, which will prevent efficient annihilation of the DM abundance. Since the direct detection signals are dominated by the vector coupling, and the

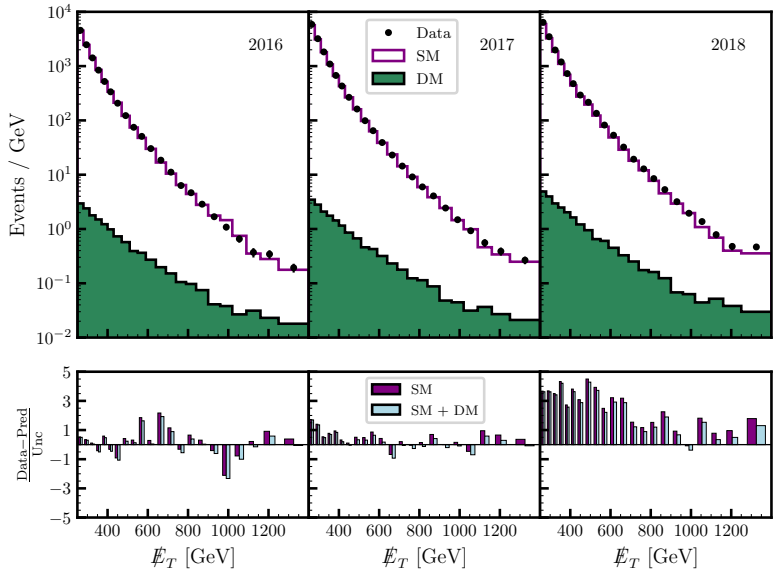

Figure 3: Spectra of missing energy for the CMS monojet search for the best-fit Dirac DM model. The lower panel shows the residuals for both the background-only and background+signal predictions.

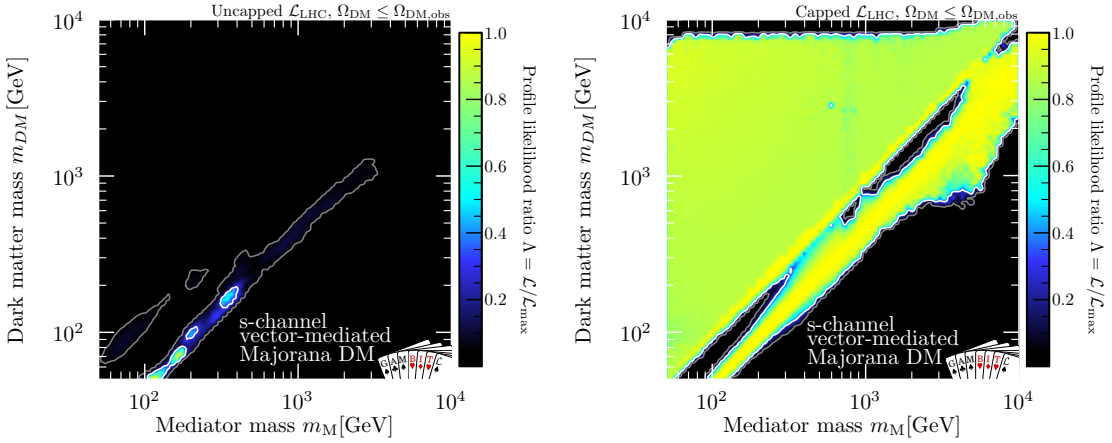

Figure 4: Profile likelihood for the Majorana fermion DM model where the model is allowed to underpredict the observed relic abundance. The collider likelihood is either capped (right) or left uncapped (left). 1σ contours are shown in white whilst 2σ contours are shown in grey.

unitarity violation arises from the axial-vector coupling, this complexity in the exclusion surface would not be present if solely allowing one of these couplings.

3.3 Majorana DM

We show the results of global scans of the Majorana fermion DM model in Figure 4. Like the Dirac DM model, fluctuations in collider data are fit by the model when the collider likelihood is not capped (left panel). The surviving parameter space in the capped collider scan is much greater than for the Dirac DM because the relevant effective operators are suppressed in the non-relativistic

limit. The slight preference toward the resonance region over the $m_{\rm DM} > m_{\rm M}$ region in the right panel is because the predicted gamma-ray flux is non-negligible when the annihilation channel into mediators is open. Since p-wave annihilation dominates at early times, this increase in annihilation cross-section is not met with a drop in the relic density fraction. The effect is that the *Fermi*-LAT data gives a preference to regions where the mediator annihilation channel is closed.

4. Conclusions

By combining constraints from dark matter and collider experiments, simplified dark models can be constrained greatly. In this talk, I have presented fits performed by the GAMBIT Collaboration of three simplified dark matter models with a spin-1 vector mediator. The surviving parameter space of all three models is split by the two annihilation channels of DM. Simultaneously including both vector and axial-vector couplings in the Dirac DM model split the off-resonance regions even further. The limits on the Majorana model are much weaker than the other two due to the suppression of non-relativistic operators. These models may be constrained well in the near future with LHC Run 3 and next-generation dark matter detectors.

Acknowledgements

I thank the organisers of the DISCRETE conference, my fellow members of the GAMBIT community for feedback and the coauthors of the article this talk is based on. This work is supported by PRACE for awarding access to Joliot-Curie at CEA, the Australian National Computational Infrastructure for access to Gadi and the Cambridge Service for Data Driven Discovery (CSD3) for access to the DiRAC HPC facility.

References

[1] Christopher Chang, Pat Scott, Tomás E. Gonzalo, Felix Kahlhoefer, Anders Kvellestad, and Martin White. Global fits of simplified models for dark matter with GAMBIT I. Scalar and fermionic models with s-channel vector mediators. preprint available at arXiv:2209.13266.

[2] D. Clowe, M. Bradač, A. H. Gonzalez, M. Markevitch, S. W. Randall, C. Jones, and D. Zaritsky. A Direct Empirical Proof of the Existence of Dark Matter. , 648:L109–L113, September 2006.

[3] Felix Kahlhoefer, Kai Schmidt-Hoberg, Thomas Schwetz, and Stefan Vogl. Implications of unitarity and gauge invariance for simplified dark matter models. *JHEP*, 02:016, 2016.

[4] G. D. Martinez, J. McKay, B. Farmer, P. Scott, E. Roebber, A. Putze, and J. Conrad. Comparison of statistical sampling methods with ScannerBit, the GAMBIT scanning module. *Eur. Phys. J. C*, 77(11):761, May 2017.

[5] D. N. Spergel, R. Bean, O. Doré, M. R. Nolta, C. L. Bennett, J. Dunkley, G. Hinshaw, N. Jarosik, E. Komatsu, L. Page, H. V. Peiris, L. Verde, M. Halpern, R. S. Hill, A. Kogut, M. Limon, S. S. Meyer, N. Odegard, G. S. Tucker, J. L. Weiland , E. Wollack, and E. L. Wright. Three-Year Wilkinson Microwave Anisotropy Probe (WMAP) Observations: Implications for Cosmology. , 170(2):377–408, June 2007.

[6] F. Zwicky. Die Rotverschiebung von extragalaktischen Nebeln. *Helvetica Physica Acta*, 6:110–127, 1933.